Electronic Research Archive

http://www.aimspress.com/journal/era

ERA, 30(5): 1898–1917.
DOI: 10.3934/era.2022096
Received: 28 September 2021
Revised: 13 January 2022
Accepted: 23 January 2022
Published: 07 April 2022

Research article

Inhibitory autapse with time delay induces mixed-mode oscillations related to unstable dynamical behaviors near subcritical Hopf bifurcation

Li Li[1] **and Zhiguo Zhao**[2,*]

[1] Guangdong Key Laboratory of Modern Control Technology, Institute of Intelligent Manufacturing, Guangdong Academy of Sciences, Guangzhou, 510070, China

[2] School of Science, Henan Institute of Technology, Xinxiang, 453003, China

* **Correspondence:** Email: zzg164637758@163.com.

Abstract: Mixed-mode oscillations (MMOs) consisting of spikes alternating with a series of subthreshold oscillations have been observed in various neurons related to some physiological functions. In the present paper, inhibitory-autapse-induced MMOs are simulated by using the Hodgkin-Huxley neuron model, and the underlying dynamical mechanism is identified to be related to dynamics of unstable behaviors near subcritical Hopf bifurcation. For the monostable spiking, a delayed inhibitory current pulse activated by a spike can suppress the phase trajectory corresponding to depolarization phase of the next spike to the unstable focus nearby or the neighborhood outside of unstable limit cycle, respectively. Then the trajectory rotates multiple cycles away and converges to the stable limit cycle, resulting in an evolution process of membrane potential from small-amplitude subthreshold oscillations to a large-amplitude spike, i.e., MMOs. For the spiking coexisting with the resting state, inhibitory autapse induces MMOs and resting state from the spiking. The difference in the MMOs from those induced by the excitatory autapse is identified. The result presents the underlying nonlinear mechanisms of inhibitory autapse to suppress the neuronal firing and reveals the potential role to control the neuronal firing patterns near subcritical Hopf bifurcation.

Keywords: inhibitory autapse; time delay; mixed-mode oscillations; subcritical Hopf bifurcation; neural firing

1. Introduction

In the nervous system, the distinct firing behaviors of neurons, such as spiking, bursting and mixed-mode oscillations (MMOs) [1], play different roles in signal transmission and processing [2]. MMOs are important rhythmic behaviors related to cellular functions, and have been observed in spinal motoneurons, pre-Bötzinger complex neurons [3,4], etc. For instance, MMOs in central pattern generators

are important for motor control. In addition, the abnormal MMOs have been found to be related to some physiological dysfunctions and diseases. For instance, during the acute intermittent hypoxia, MMOs-like rhythmic activities in pre-Bötzinger complex have been observed. This suggests that MMOs are related to some diseases including acute respiratory distress syndrome, obstructive sleep apneas, myocardial infarct, and sudden infant death syndrome [3]. To obtain the generation mechanism, MMOs have been studied by model analysis and simulations, and the researches focus on the multiple-time-scales characteristics of neural systems in the nonlinear dynamical process. The interactions of ionic currents with different time scales were found to play critical roles in triggering MMOs for single neurons [5–8]. For example, MMOs appearing in the entorhinal cortex stellate neuron were found to involve the participation of fast- and slow-activating hyperpolarization-activated currents [5]. The slow inactivation of sodium current and slow activation of potassium current was found to lead to the generation of MMOs [6].

Besides the interactions of ionic currents, synaptic inputs can also lead to the generation of MMOs in single neurons or neural networks. For example, owing to the neuronal synaptic interactions, MMOs appear in coupled FitzHugh-Nagumo neurons [9] and the excitatory neural network of the pre-Bötzinger complex [3]. Excitatory self-feedback can change the periodical spiking of neurons near subcritical Hopf bifurcation to MMOs [10]. Moreover, synaptic input is an important factor that determines neuronal activities, and is classified as excitatory input or inhibitory input based on the opposite effects on membrane potential. It is commonly assumed that inhibitory inputs suppress firing activities whereas excitatory inputs facilitate firing activities [11]. Fast excitatory synaptic coupling usually promotes the synchronization of neuronal firing whereas fast inhibitory inputs desynchronize neuronal firing [12]. However, the novel effects of excitatory and inhibitory synapses different from the above-mentioned phenomena have been observed. For instances, inhibitory stimulation was found to facilitate membrane potential to approach the threshold of action potential through post-inhibitory rebound [13]. Excitatory coupling in neuronal networks can desynchronize the neuronal firing activities, and inhibitory coupling can synchronize the neuronal firing activities when the synaptic decay constant is small or small delay is considered [12].

Autapse is a special synapse that connects the axon and dendrite of one neuron, and has been observed in experiments [14]. Through the experimental studies, excitatory autapses have been documented in Golgi-stained neocortical neurons, neocortical layer 5 pyramidal neurons and motor neurons, and inhibitory autapses have been identified from inhibitory interneurons in cerebellum, visual cortex and neocortex [10, 14]. Furthermore, some functions on the two autapses have also been identified in the electrophysiological experiments. For instances, excitatory autapse facilitates burst firing and enhances the coincidence detection of pyramidal neurons in the neocortex [15]. Inhibitory autapse can enhance the spike-timing precision of the fast-spiking interneurons in the neocortex to improve temporal coding [14]. Excitatory autapse can induce the persistent firing of motor neuron in Aplysia buccal ganglia due to its positive role in spike generation [16], whereas inhibitory autapse suppress the repetitive firing of neocortical interneurons owing to its negative role [14]. Besides these biological experiments, more potential functions of autapse have been identified in theoretical model computations [18–20]. For example, the autapse was shown to play important roles on modulating neuronal electrical activities such as the firing patterns of single neurons [21,22], and the collective behaviors for neuronal networks such as resonance [23]. The excitatory autapse contributes to irregular/chaotic and burst firing patterns, whereas the inhibitory autapse suppresses these patterns [21, 22]. In addition, ex-

citatory and inhibitory autapses without time delay exhibit opposite effects on the changes of neuronal excitability. For instance, the excitatory autapse can induce neuronal excitability changing from class II to class I, whereas the inhibitory autapse can induce the change from class I to class II [24]. When time delay in excitatory autapse is considered, neuron is changed from class I and III excitabilities to class II excitability [25]. Furthermore, some counter-intuitive effects of inhibitory and excitatory autapse on neuronal electrical activities have been shown, especially for class II excitability of neurons existing extensively in the nervous systems [10, 26]. For instance, the inhibitory autapse can induce an increase in the spike number in burst for bursting neurons, while the excitatory autapse can reduce the spike number [27, 28]. For neurons with class II excitability, the inhibitory autapse can change the resting state to repetitive spiking via the elicitation of the post-inhibitory rebound spike [26]. Moreover, the excitatory autapse with a suitable time delay can induce periodic spiking near subcritical Hopf bifurcation (corresponding to class II excitability) changes as MMOs [10], which leads to the reduction of the firing frequency.

Based on the above findings, the inhibitory autapse/synapse and excitatory autapse/synapse usually have different effects on neuronal firing and the collective behaviors of the neuronal network, or have similar effects under different conditions. The excitatory autapse can induce MMOs near the subcritical Hopf bifurcation, and whether the inhibitory autapse can induce MMOs is not known yet. In addition, the dynamical mechanism for the suppression effects of inhibitory autapse on repetitive spiking has been observed in electrophysiological experiment [14], remains unclear. In this paper, we present the effects of an inhibitory autapse on the periodic spiking of the classic Hodgkin-Huxley (HH) model, and consider two regions with different dynamical behaviors (monostable spiking, coexistence of spiking and resting state) near the subcritical Hopf bifurcation. For the two regions, the inhibitory autapse can change the firing pattern from periodic spiking to regular or irregular MMOs by modulating the time delay, and can also cause resting state changing from periodic spiking in the bistable region. Apart from these, the distinctions of the MMOs in these two regions are shown. The similarity and difference between the dynamical mechanisms for the MMOs induced by the inhibitory autapse and excitatory autapse are discussed. The results indicate that the inhibitory autapse has more potential functions in neuronal systems, and provide a deeper understanding for the suppression effect of inhibitory autapse observed in experiment [14].

The paper is organized as follows. In section 2, the models of the classic HH neuron and autaptic HH neuron are given. In section 3, it is presented that the inhibitory autapse induces the regular and irregular MMOs changing from periodic spiking in monostable and bistable regions. The changing mechanism for these dynamical behaviors is obtained through phase plane analysis. In addition, based on the generation mechanism of the MMOs, the resting state induced by the inhibitory autapse is simulated. Discussions and conclusions are given in the last section.

2. Model and methods

2.1. Model

In this paper, the conductance-based HH model with inhibitory autapse is investigated to explore the different effects of the inhibitory autapse on the responses of neuron near the subcritical Hopf bifurcation. The HH neuron model with autaptic current [26] is:

$$C\frac{dV}{dt} = -I_{Na} - I_K - I_L + I_{stim} - I_{aut}, \tag{2.1}$$

where C and V are membrane capacitance and potential, respectively, t denotes time, I_{Na}, I_K, I_L, and I_{aut} represent the sodium, potassium, leakage, and autaptic currents, respectively, I_{stim} is the constant stimulated current. The related expressions are given by $I_{Na} = \overline{g}_{Na}m^3h(V - E_{Na})$, $I_K = \overline{g}_K n^4(V - E_K)$, $I_L = \overline{g}_L(V_L - E_L)$ and $I_{aut} = g_{aut}(V - E_s)\Gamma(V(t-\tau))$ with $\Gamma(V(t-\tau)) = 1/(1+\exp(-10(V(t-\tau)-V_{thres})))$, respectively, where m and h denote the activation and inactivation variables of I_{Na}, respectively, and n denotes the activation variable of I_K. The variables m, h, and n satisfy:

$$\frac{dm}{dt} = \alpha_m(1 - m) - \beta_m m, \tag{2.2}$$

$$\frac{dh}{dt} = \alpha_h(1 - h) - \beta_h h, \tag{2.3}$$

$$\frac{dn}{dt} = \alpha_n(1 - n) - \beta_n n, \tag{2.4}$$

with $\alpha_m(V) = 0.1(V + 10)/(1 - \exp(-0.1(V + 40)))$, $\beta_m(V) = 4\exp(-(V + 65)/18)$, $\alpha_h(V) = 0.07\exp(-(V+65)/20)$,$\beta_h(V) = 1/(1+\exp(-0.1(V+35)))$, and $\alpha_n(V) = 0.01(V+55)/(1-\exp(-0.1(V+55)))$, $\beta_n(V) = 0.125\exp(-(V + 65)/80)$. In the expression of the autaptic current I_{aut} in Eq (2.1), g_{aut} represents the coupling strength of the autapse, τ describes the time delay in information transmission between the dendrite and axon. In this paper, the influence of the inhibitory autapse and stimulated current I_{stim} on the dynamical behaviors of the HH neuron is studied. The values and representations of the fixed parameters are given in Table 1. Hereafter, the HH neuron without the autaptic current will be called the classic HH neuron model, and the HH neuron with the autaptic current will be referred to as the autaptic HH neuron model.

Table 1. Parameters for the autaptic HH neuron model.

Parameters	Values	Representations
C	$1\mu F/cm^2$	Membrane capacitance
g_{Na}	$120\mu S/cm^2$	Maximum conductance of I_{Na}
E_{Na}	$50mV$	Reversal potentials of I_{Na}
g_K	$36mS/cm^2$	Maximum conductance of I_K
E_K	$-77mV$	Reversal potentials of I_K
g_L	$0.3mS/cm^2$	Maximum conductance of I_L
E_L	$-54.4mV$	Reversal potentials of I_L
E_s	$-80mV$	Reversal potentials of I_{aut}
V_{thres}	$-15mV$	Threshold of I_{aut}

2.2. Methods

We performed the simulation of the classic HH neuron model and the autaptic HH neuron model through the methods of Runge-Kutta with 0.01 ms step size. The bifurcation diagram (Figure 1(a)) is obtained by using the AUTO in XPPAUT [29]. The initial history for simulating the autaptic HH neuron model is selected from the stable spiking of the classic HH neuron model.

3. Results

3.1. Bifurcations for the classic HH neuron model

Figure 1(a) displays a bifurcation diagram, in which the membrane potential V changes with the stimulated current I_{stim} for the classic HH neuron (HH neuron without autaptic current). It can be seen that the fold bifurcation of limit cycles (FLC, magenta solid circles) and subcritical Hopf bifurcation (SubH, green solid circle) in the diagram. The FLC occurs at $I_{stim} \approx 6.26\,\mu$A/cm^2, which separates the stable limit cycle (blue solid circle) from unstable limit cycle (blue hollow circle). The SubH appears at $I_{stim} \approx 9.78\,\mu$A/cm^2, wherein the stable focus (red solid line) switches to the unstable limit cycle (blue hollow circles). The stable limit cycle is on the right side of the bifurcation point SubH, which corresponds to stable repetitive spiking. Moreover, the stable limit cycle and focus coexist within the region between the bifurcation points FLC and SubH, which correspond to the stable repetitive spiking and stable resting state, respectively. As we know, the change in neurons from the resting state to repetitive spiking via Hopf bifurcation corresponds to class II excitability. The classic HH neuron exhibits class II excitability, and Figure 1(b) shows the firing frequency curve.

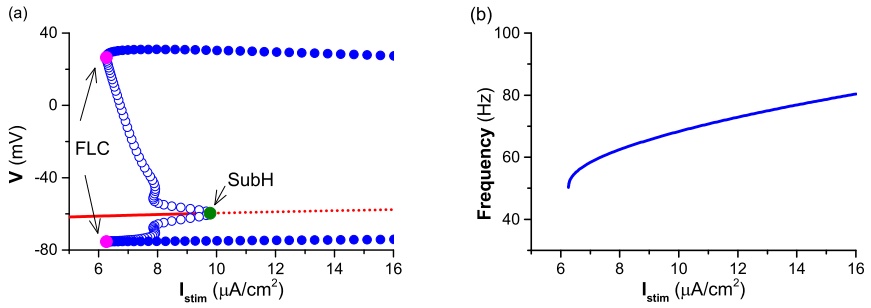

Figure 1. The effects of the stimulated current I_{stim} on the classic HH neuron (HH neuron without autaptic current). (a) The bifurcations with respect to I_{stim}. The blue solid (hollow) circles symbolize the stable (unstable) limit cycle. The magenta and green solid circles are the bifurcation points FLC and SubH, respectively. The red solid (dotted) line denotes the stable (unstable) focus; (b) The firing frequency with respect to I_{stim}.

The dynamical behaviors on both sides of the bifurcation point SubH, the monostable spiking region or bistable region of spiking and resting state, are different for the classic HH neuron model. In this paper, the effects of the inhibitory autapse on spiking in these two regions near the bifurcation point SubH are considered.

3.2. Inhibitory-autapse-induced MMOs

In this subsection, inhibitory-autapse-induced MMOs changing from periodic spiking in the monostable or bistable regions are given. It is found that MMOs can be induced by changing the coupling strength and time delay in inhibitory autapse for these two regions.

3.2.1. MMOs induced from coexisting spiking

For the periodic spiking in the bistable region of the classic HH neuron, the firing patterns of the HH neuron can be changed as MMOs through introducing the inhibitory autapse. When the initial values are chosen from outside of the unstable limit cycle, the steady state is periodic spiking. For instance, when $I_{stim} = 9.6\,\mu$A/cm^2, Figure 2(a) and (c) show the spike train (blue solid line) and its phase trajectory, respectively, for the classic HH neuron model. The corresponding firing frequency is about 67.279 Hz. Still chosen the same initial values, when an inhibitory autapse with the coupling

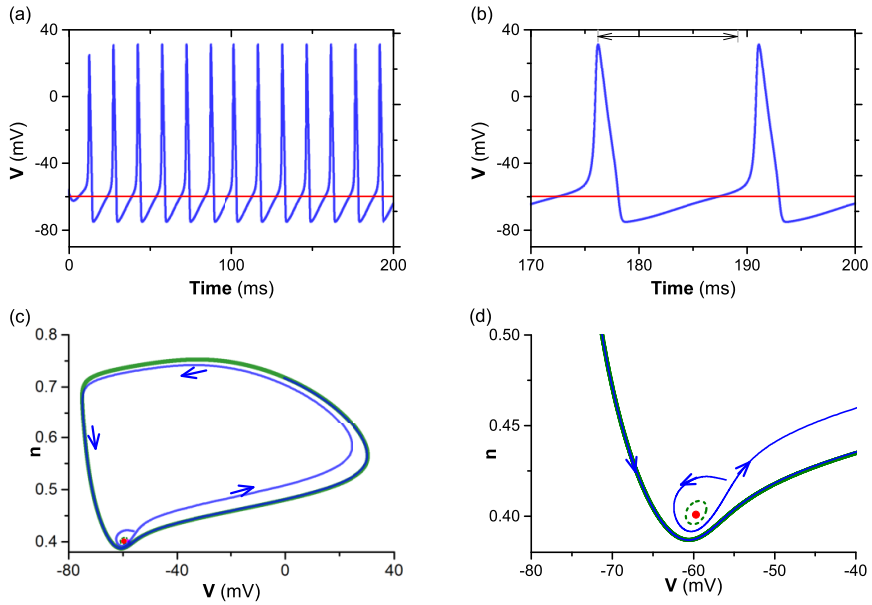

Figure 2. The periodic spiking (blue curve) coexisting with resting state (red curve) for the classic HH neuron when $I_{stim} = 9.6\,\mu$A/cm^2. (a) Spike train. (b) Enlargement of (a). (c) Phase portrait of (a). (d) Enlargement of (b) around the unstable limit cycle. Blue solid curves in (b) and (c) are the trajectories corresponding to the membrane potential in (a). The green solid (dashed) curve is the stable (unstable) limit cycle. The red solid circle represents the stable focus. The arrows denote the direction of the trajectory.

strength $g_{aut} = 0.15$ mS/cm^2 and time delay $\tau = 12.6$ ms is introduced, the firing pattern changes to MMOs that are composed of small-amplitude oscillations (black solid line) and a larger-amplitude spike (blue solid line), as shown in Figure 3(a) and (b). The average firing frequency of the MMOs (24.516 Hz) is far below that of periodic spiking (67.279 Hz) of the classic HH neuron, which indicates that the inhibitory autapse suppresses neural firing. By comparing the two different firing patterns, it is found that the small-amplitude oscillations induced by the inhibitory autapse can enlarge the regions of the two adjacent spikes and make the firing frequency lower. The delayed inhibitory autaptic current (magenta dashed curve) activated by a spike plays a role in the depolarization phase (cyan curve) after the spike due to the existence of time delay ($\tau = 12.6$ ms), and can suppress the spike to induce small-amplitude oscillations.

To reveal the generation mechanism of small-amplitude oscillations induced by the inhibitory autaptic current, the phase portrait corresponding to Figure 3(a) is depicted in Figure 3(c). The trajectory

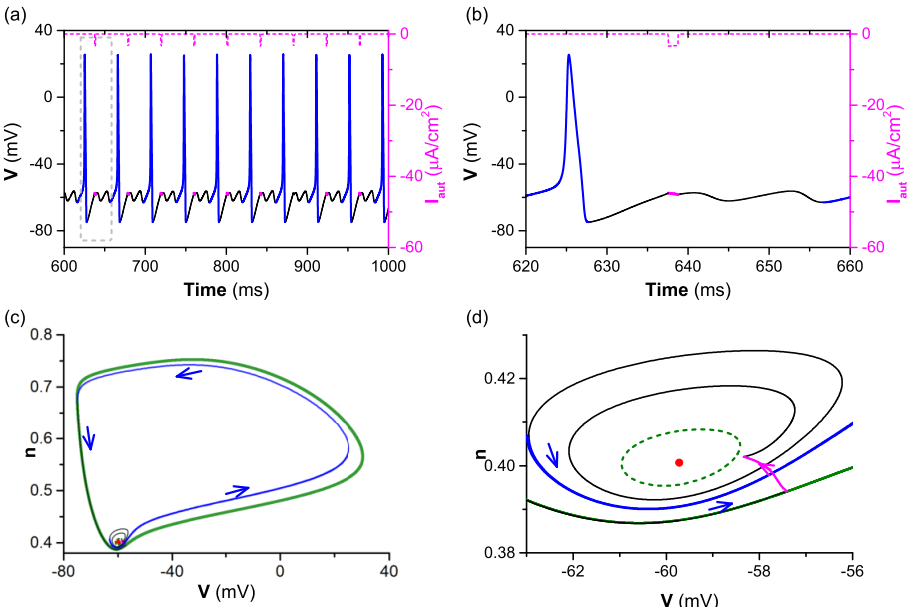

Figure 3. Inhibitory-autapse-induced MMOs when $I_{stim} = 9.6\,\mu$A/cm^2, $g_{aut} = 0.15$ mS/cm^2, and $\tau = 12.6$ ms. (a) MMOs. Black solid curves represent the small-amplitude oscillations, and blue solid curves represent the large-amplitude spikes. The magenta dashed curve is the inhibitory autaptic current, and the magenta solid curve is the corresponding membrane potential. The cyan solid is the depolarization phase. (b) Enlargement of the gray dashed box in (a). (c) Projection of trajectory corresponding to the membrane potential in (b). The green solid (dashed) curve corresponds to the (unstable) stable limit cycle of the classic HH model. The red solid circle represents the stable focus for the classic HH model. The trajectories are marked with colors that are the same as those of the membrane potential in (a). The arrows denote the direction of trajectory. (d) Enlargement of (c).

(blue solid line) rotates counterclockwise along the stable limit cycle (green solid curve). When it evolves to the lower right of the unstable limit cycle (green dashed curve), the trajectory (magenta solid line part) affected by the delayed inhibitory autaptic current is suppressed to the neighboring outside of the unstable limit cycle. Begin with when the inhibitory autaptic action ends, the evolution of the trajectory is determined by the intrinsic characteristic of the classic HH neuron. The trajectory (black solid curve) rotates away from the unstable focus, and converges to the stable limit cycle. Then, small-amplitude oscillations (black solid curve) with gradually increasing amplitudes are generated during the multiple rotations. However, before the phase trajectory reaches the stable limit cycle, one large spiral curve (blue solid curve) corresponding to spiking is formed, which reactivates the inhibitory autaptic current that can resuppress the trajectory to the outside of the unstable limit cycle, and form the small-amplitude oscillations. Repeating the above processes, subthreshold oscillations and spiking appear alternately, i.e., MMOs.

3.2.2. MMOs induced from monostable spiking

For the monostable region of the classic HH neuron, the inhibitory autapse can also change its firing patterns from periodic spiking to MMOs. In the monostable region, the classic HH neuron exhibits periodic spiking, for example, the membrane potential (green solid line) evolves to the stable periodic spiking when $I_{stim} = 10\,\mu$A/cm^2, shown in Figure 4(a), and the corresponding trajectory is the stable limit cycle, shown in Figure 4(b). The firing frequency is about 68.31 Hz.

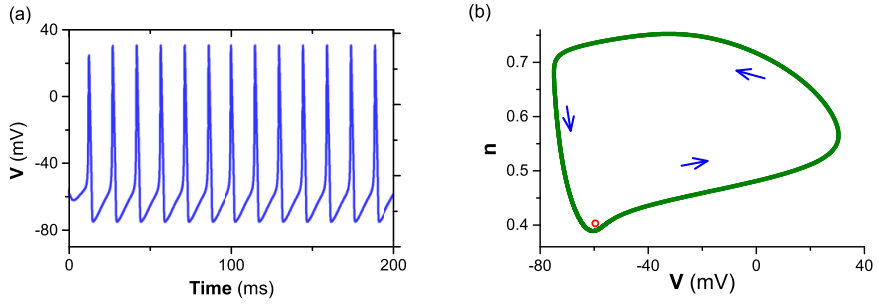

Figure 4. Monostable periodic spiking for the classic HH neuron when $I_{stim} = 10\,\mu$A/cm^2. (a) Spike train. (b) Phase portrait of (a). Blue solid curve in (b) is the trajectory corresponding to the membrane potential in (a). Green solid curve represents the stable limit cycle. The red hollow circle represents the unstable focus.

When the inhibitory autapse with the coupling strength $g_{aut} = 0.2$ mS/cm^2 and time delay $\tau = 12.6$ ms is introduced into the classic HH model, the firing pattern becomes MMOs, shown in Figure 5(a) and (b). The mean firing frequency (15.4 Hz) is much lower than that (68.31 Hz) of the periodic spiking for the classic HH neuron, which means that the inhibitory autapse can suppress neuronal firing. Similar to the MMOs for the bistable region (Figure 3), the delayed inhibitory autaptic current has a great effect on the depolarization phase after a spike to induce small-amplitude oscillations. The small-amplitude oscillations enlarge the interspike region to lower firing frequency.

To reveal the generation mechanism of the small-amplitude oscillations, the phase portrait of the membrane potential shown in Figure 5(a) is depicted in Figure 5(c). The phase trajectory (blue solid line) rotates the stable limit cycle counterclockwise, and evolves to the lower right of the unstable focus,

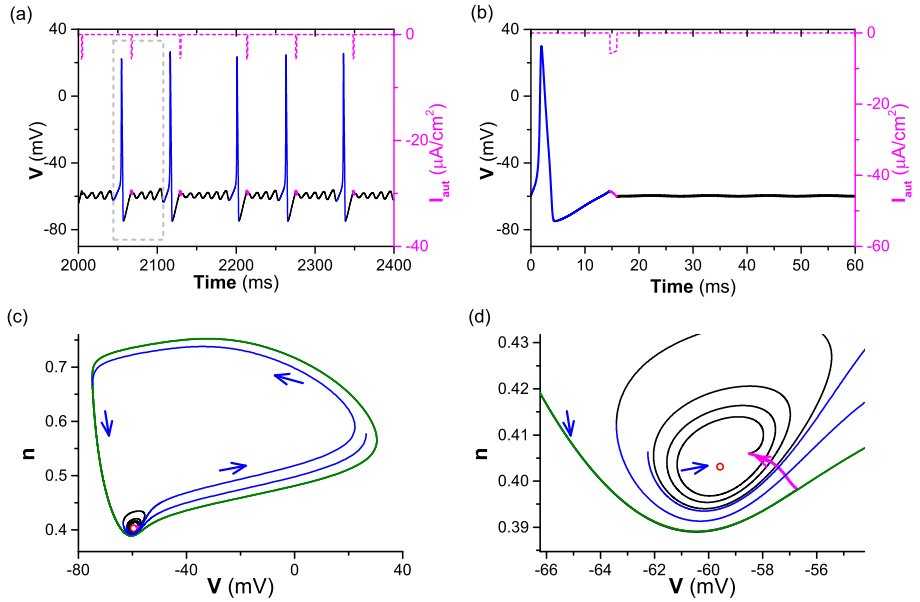

Figure 5. Inhibitory-autapse-induced MMOs when $I_{stim} = 10\,\mu$A/cm^2, $g_{aut} = 0.2$ mS/cm^2, and $\tau = 12.6$ ms. (a) The train of MMOs. Black (blue) solid curves are subthreshold oscillations (spikes). The magenta dashed curve is the inhibitory autaptic current, and the magenta solid curve is the corresponding membrane potential. (b) Enlargement of gray dashed box in (a). (c) Projection of the trajectory corresponding to the membrane potential in (b). The green solid curve corresponds to the stable limit cycle for the classic HH model. The red solid circle represents stable focus for the classic HH model. The trajectories are marked with colors that are the same as those of membrane potential in (a). The arrows denote the direction of trajectory. (d) Enlargement of (c).

which is suppressed by the inhibitory synaptic current to the region close to the unstable focus. After the inhibitory synaptic current, the revolution of the phase trajectory is determined by the classic HH neuron, and the phase trajectory (black solid line) will spirally converge to the stable limit cycle through several rotations and generate the subthreshold oscillations with the increasing amplitude. However, before the phase trajectory reaches the stable limit cycle, a spiral line (blue solid line) with larger amplitude is formed, which corresponds to a spike that can activate the inhibitory autaptic current, and the current resuppresses the trajectory to the outside near the unstable limit cycle to generate small-amplitude oscillations. Repeating the above processes, the firing pattern of the MMOs can be formed.

By comparing the patterns of MMOs induced by the inhibitory autapse for the bistable region with the monostable region (Figure 3), it is found that the minimal amplitude of small-amplitude oscillations induced by the inhibitory autapse is relatively small and the mean firing frequency of MMOs is relatively large for the monostable region. The inhibitory autaptic current can suppress the phase trajectory to the nearby outside of the unstable limit cycle for the bistable region, and the unstable focus for the monostable region, respectively. The unstable behaviors where the trajectory will be suppressed are different, the phase trajectory perturbed by the inhibitory autaptic current for the MMOs in the monostable spiking region rotates more cycles before converging to a spike with larger amplitude, and the minimum of the small-amplitude oscillations induced by inhibitory autapse is smaller than the trajectory for MMOs in the bistable region.

3.3. Effect of time delay on the changes of dynamical behaviors

3.3.1. Effect on periodic spiking in the monostable region

To show how the effects of time delay on the generation of the MMOs, we present bifurcations of ISI with respect to time delay for the autaptic HH model. For example, when $I_{stim} = 10\,\mu$A/cm^2 (in the monostable region) and $g_{aut} = 0.2$ mS/cm^2, the bifurcation diagrams of ISI are shown in Figure 6(a) and (b).

The dynamical behavior of the HH neuron is periodic spiking for $\tau < 12.03$ ms. For example, when $\tau = 10$ ms, periodic spiking and its trajectory in phase plane (V, m) are shown in Figure 7(a1) and (a2), respectively. When $\tau = 12.03$ ms, irregular MMOs appear. For example, when $\tau = 12.04$ ms, irregular MMOs and their trajectories are shown in Figure 7(b1) and (b2), respectively. As τ increases further, periodic and irregular MMOs appear alternately. For example, the periodic MMOs appear for $\tau \in (12.129, 12.144) \cup (12.383, 12.392) \cup (12.431, 12.461) \cup (12.48, 12.509) \cup (12.904, 13)$. When $\tau = 12.13$ ms and $\tau = 12.44$ ms, the time course of the periodic MMOs and its trajectory in phase plane (V, m) is shown in Figure 7(c) and (e), respectively. For example, the irregular MMOs appear for $\tau \in (12.03, 12.128) \cup (12.145, 12.382) \cup (12.393, 12.47) \cup (12.462, 12.47) \cup (12.51, 12.905)$, when $\tau = 12.2$ ms, the time course of the irregular MMOs and its trajectory is shown in Figure 7(d). In the end, the dynamical behavior returns to periodic spiking. For instance, when $\tau = 13.1$ ms, the periodic spiking is shown in Figure 7(f).

3.3.2. Effect on periodic spiking in the bistable region

When $I_{stim} = 9.6\,\mu$A/cm^2 (in the bistable region), the bifurcation diagrams are shown in Figure 6(c) and (d). Similar to the monostable region, the inhibitory autapse induces transitions between regular and irregular MMOs as time delay increases.

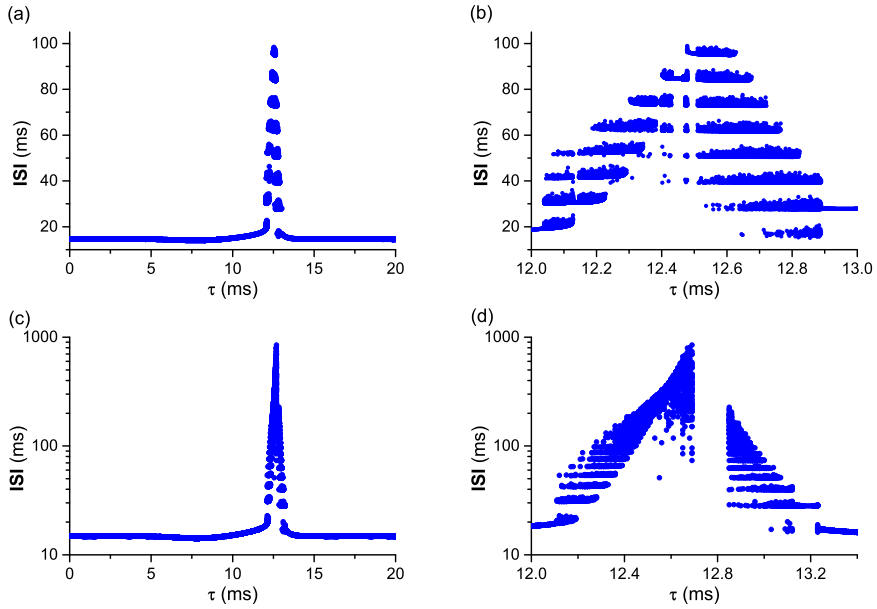

Figure 6. Changes of ISI with respect to time delay when I_{stim} and g_{aut} at different values. (a) $I_{stim} = 10\,\mu$A/cm^2 and $g_{aut} = 0.2$ mS/cm^2. (b) The enlargement of (a). (c) $I_{stim} = 9.6\,\mu$A/cm^2 and $g_{aut} = 0.2$ mS/cm^2. (d) is the enlargement of (c).

3.4. Inhibitory-autapse-induced resting state from spiking in the bistable region

In Figure 6(c) and (d), there is no ISI for $\tau \in (12.7, 12.84)$, which indicates that some subthreshold activities may be induced by the inhibitory autapse in the region. As can be seen from Figure 3, the trajectory perturbed by the inhibitory autaptic current may pass over the unstable limit cycle and stay inside the unstable limit cycle, which leads to resting state, i.e., the inhibitory autapse induces resting state changing from spiking in the bistable region. For example, when $I_{stim} = 9.6\,\mu$A/cm^2, the initial values are chosen to be the same as Figure 2(a), and an inhibitory autapse with $g_{aut} = 0.25$ mS/cm^2 and $\tau = 13$ ms is introduced, the membrane potential evolves to the resting state (red solid line) via a spike (blue solid curve) and damping oscillations (black solid line), shown in Figure 8(a) and (b). The trajectory corresponding to the membrane potential in Figure 8(a) is shown in Figure 8(c) and (d). The evolution of the trajectory is similar to Figure 3(c) and (d) except that the trajectory (magenta solid line) passes over the unstable limit cycle (green dashed line).

3.5. Different dynamical behaviors on the parameter plane (g_{aut}, τ)

In addition to time delay τ, the autaptic strength g_{aut} plays important roles in the generation of different dynamical behaviors, including MMOs and resting state. To clearly show the effects of g_{aut} and τ on the periodic spiking of the classic HH neuron, the distributions of different firing patterns on the parameter plane (g_{aut}, τ) are shown in the left panels of Figure 9. The corresponding average firing frequency is presented in the right panels of Figure 9. When I_{stim} is located in the bistable region of the classic HH neuron, for example, $I_{stim} = 9\,\mu$A/cm^2 and $I_{stim} = 9.6\,\mu$A/cm^2, the distributions are shown in Figure 9(a) and (b), respectively. When I_{stim} is located in the monostable region, for example, $I_{stim} = 9.8\,\mu$A/cm^2 and $I_{stim} = 10\,\mu$A/cm^2, the distributions are shown in Figure 9(c), and (d),

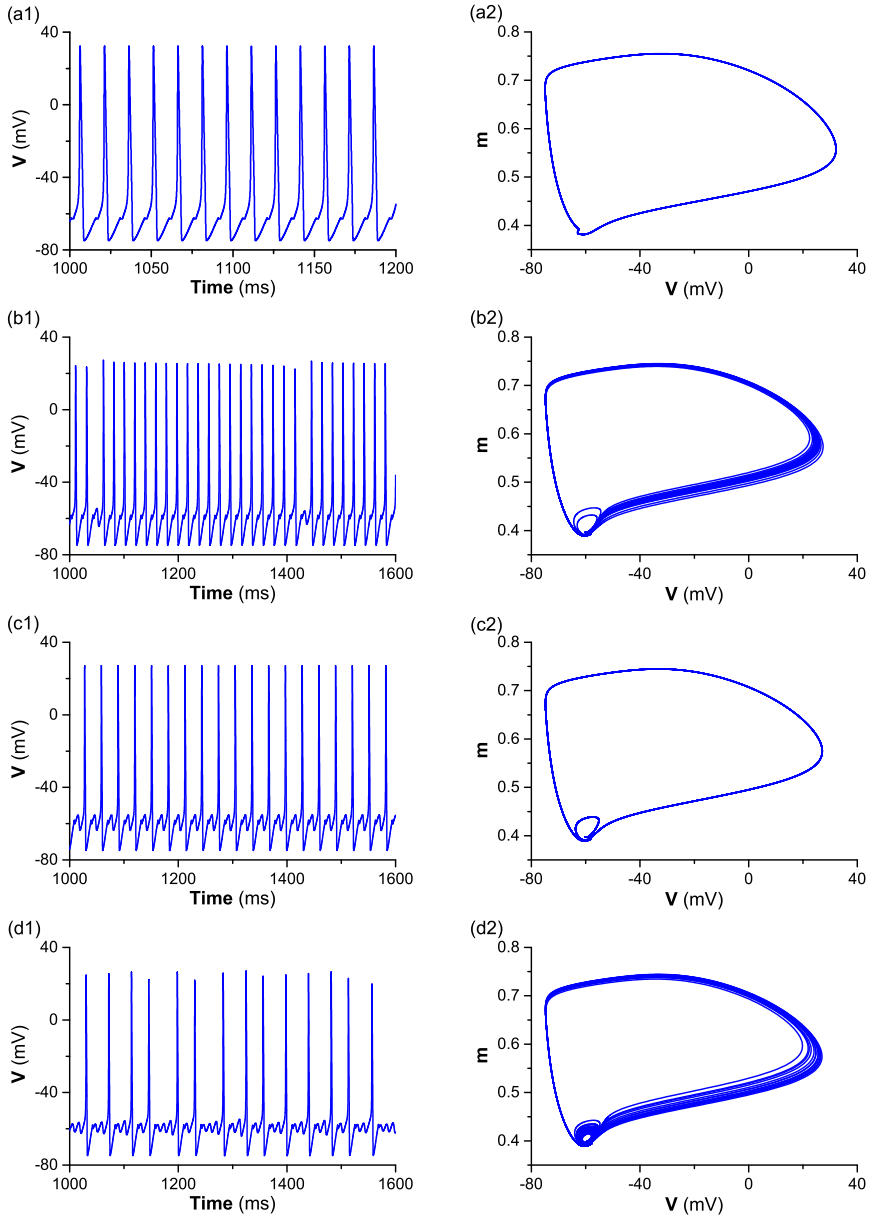

Figure 7. (Figure continued on next page)

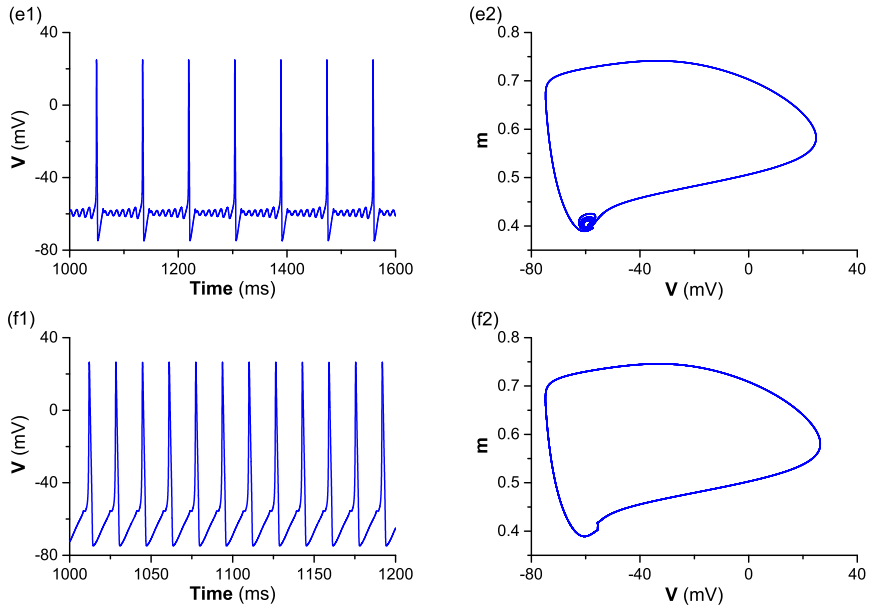

Figure 7. Different dynamical behaviors at different values of time delay when I_{stim} = 10 μA/cm^2 and g_{aut} = 0.2 mS/cm^2. (a1) and (a2) Regular spiking when τ = 10 ms; (b1) and (b2) Irregular MMOs when τ = 12.04 ms; (c1) and (c2) Regular MMOs when τ = 12.13 ms; (d1) and (d2) Irregular MMOs when τ = 12.2 ms; (e1) and (e2) Regular MMOs when τ = 12.44 ms; (f1) and (f2) Regular spiking when τ = 13.1 ms. Left panels: Time course of membrane potential, Right panels: Trajectory corresponds to the left panels in the phase plane (V,m).

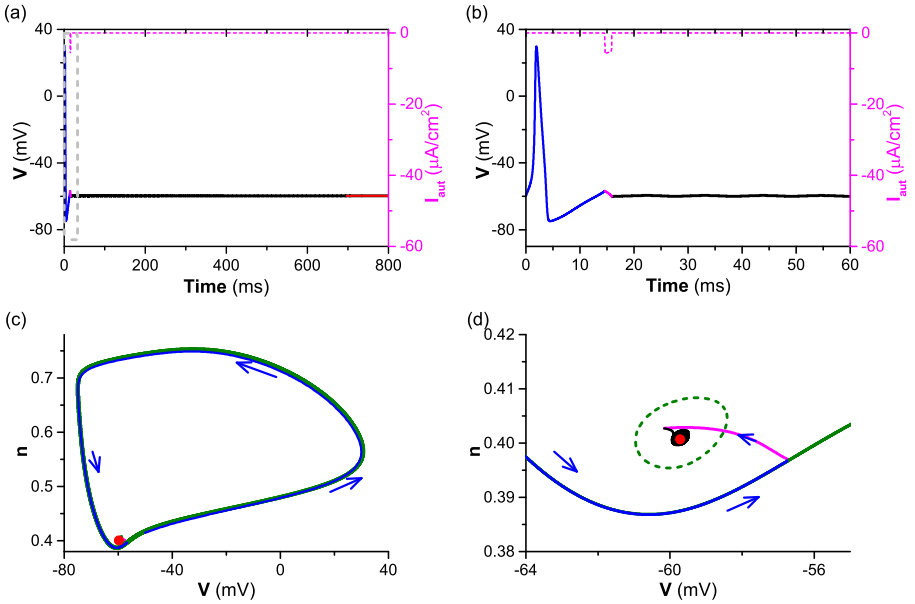

Figure 8. Inhibitory-autapse-induced resting state when I_{stim} = 9.6 μA/cm^2, g_{aut} = 0.2 mS/cm^2, and τ = 12.6 ms. (a) Resting state (red) following subthreshold oscillations (black) and spikes (blue). The magenta dashed curve is the inhibitory autaptic current. The magenta solid curve is the corresponding membrane potential. (b) Enlargement of gray dashed box in (a). (c) Projection of the trajectory corresponds to the membrane potential of (b). The green solid (dashed) curve corresponds to the stable (unstable) limit cycle for the classic HH model. The red solid circle represents the stable focus for the classic HH model. The trajectories are marked with colors that are the same as those of the membrane potential in (a). The arrows denote the direction of the trajectory. (d) Enlargement of (c).

respectively. In the left panels of Figure 9, the dynamical behaviors in the white, red and blue regions are resting state, MMOs and periodic spiking, respectively. In the right panels of Figure 9, different colors denote the average firing frequency.

For the bistable region, the inhibitory autapse can induce MMOs and resting state changing from periodic spiking. The resting state appears in a narrow region of time delay ($\approx$ 13 ms), which is surrounded by the region for MMOs. With the increase of I_{stim}, the region of the resting state shrinks and the region of MMOs enlarges. The shrinking of the region of the resting state (Figure 9(a) and (b)) is due to the decreases of the amplitude of the unstable limit cycle with the increase of I_{stim} (Figure 1(a)).

For the monostable region, the inhibitory autapse can induce MMOs changing from periodic spiking, however, it cannot induce resting state, as shown in Figure 9(c) and (d). MMOs also appear in the narrow region of time delay around 13 ms, and their region decreases with the increase of I_{stim}.

For these two regions, MMOs or resting state appears at $\tau \approx 13$ ms. Only when the inhibitory autaptic current is applied at the depolarization phase near the resting state (the trajectory is located in the lower right of the stable focus or unstable limit cycle), MMOs or resting state can be induced. To ensure that the inhibitory autaptic current activated by the action potential is applied to the depolarization phase of the forthcoming action potential, τ is taken around 13 ms, which can be estimated by the time difference between the peak of the action potential of the classic HH neuron and the initial depolarization phase of the next action potential (double arrows in Figure 2(b), $\approx$ 12.5 ms). In Figure 9, the range of τ is roughly taken within an oscillatory period (around 14.6 ms) of the spiking of the classic HH neuron. Similar to the previous study [20] that the firing rate and firing behaviors change with time delay periodically, the MMOs and the resting state induced by inhibitory autapse also appear periodically with the increase of τ, and the period of τ is about that of the spiking of the classic HH neuron model (not shown here). A previous study [10] showed that the excitatory autapse can cause MMOs or resting state near SubH for HH neuron at smaller time delay than inhibitory autapse, which is caused by the opposite effects of inhibitory and excitatory currents on membrane potential. By modulating time delay, the excitatory autaptic current is applied at the hyperpolarization phase (the corresponding trajectory locates in lower left of the stable focus or unstable limit cycle in Figure 3(d) and Figure 5(d)) that precedes the depolarization phase, which means that time delay of excitatory autapse that can induce MMOs and resting state is smaller than that of the inhibitory autapse.

4. Conclusions

MMOs are important rhythmic firing activities in nervous system, and have been observed to implement cellular functions in many neurons [3]. The generation mechanism of MMOs is more complex than spiking and bursting, and has yet to be fully understood and classified [1]. In this paper, regular and irregular MMOs induced by the inhibitory autapse in both monostable and bistable regions near subcritical Hopf bifurcation are simulated. The generation mechanism of different MMOs caused by inhibitory autapse is identified through phase plane analysis. In addition, the resting state induced by the inhibitory autapse is found and analyzed in the bistable region.

Previous experiment had demonstrated the negative effects of inhibitory autapse on repetitive firing [14]. In addition to the negative effects, the intrinsic properties of neuron may also influence the suppression effects. That is, the suppression effects of the inhibitory autapse on neuronal activities depend on not only the negative effects of the inhibitory autaptic current but also the dynamics of the

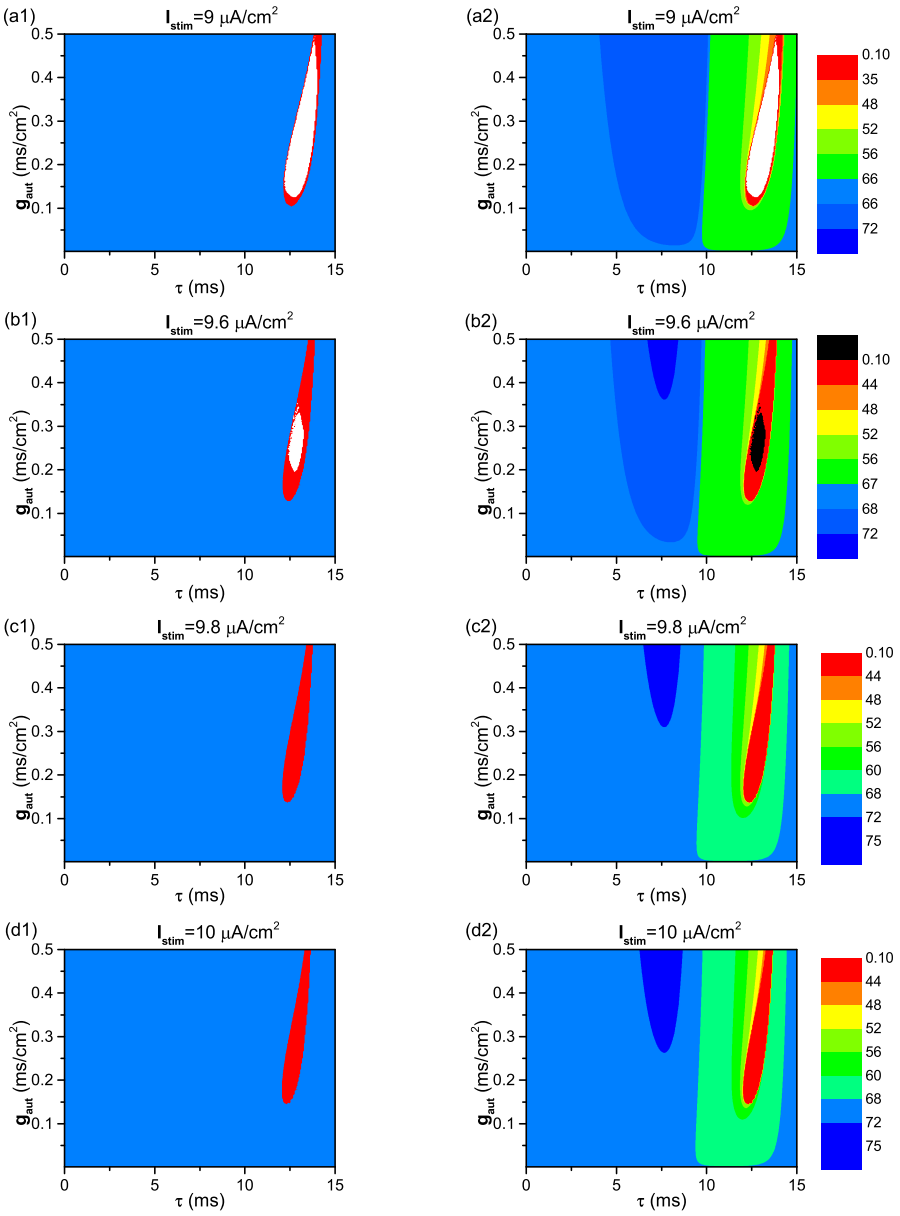

Figure 9. Effects of g_{aut} and τ on the neuronal activities and average firing frequency when I_{stim} is at different values: (a) $I_{stim} = 9\,\mu$A/cm^2; (b) $I_{stim} = 9.6\,\mu$A/cm^2; (c) $I_{stim} = 9.8\,\mu$A/cm^2; (d) $I_{stim} = 10\,\mu$A/cm^2. Left panels: distribution of different neuronal activities, neuronal activities in the white, red and blue regions are resting state, MMOs, and periodic spiking, respectively. Right panels: Distribution of average firing frequency, where the colorful scale represents the average firing frequency.

individual neuron. For the monostable region, the inhibitory autapse can induce MMOs changing from periodic spiking, and the pulse-like inhibitory autaptic current suppresses the trajectory (corresponding to the depolarization phase) to the neighborhood of the unstable focus. After the current, the trajectory rotates away from the unstable focus to converge to the stable limit cycle. During the process of rotation, the membrane potential can be gradually changed from small-amplitude subthreshold oscillations to a large-amplitude spike, i.e., MMOs are formed. For the bistable region, the inhibitory autapse can induce MMOs changing from periodic spiking, and the dynamical mechanism is similar to the situation in the monostable region, except that the initial parts of small-amplitude oscillations are near the outside of the unstable limit cycle. The different unstable behaviors cause the different firing frequency and minimum amplitude of the MMOs induced by the inhibitory autapse for the two regions. Moreover, the inhibitory autapse can cause resting state changing from periodic spiking in the bistable region, the inhibitory current could suppress the trajectory (corresponding to the depolarization phase) into the unstable limit cycle, and then the trajectory will converge to the stable focus corresponding to the resting state.

The previous study [10] showed that excitatory autapse can induce MMOs and resting state to suppress neuronal firing, which provides a paradoxical phenomenon where excitatory inputs have negative effects on neuronal firing and a potential physiological function. However, in neural systems, inhibitory synaptic input usually plays different roles from excitatory synaptic inputs in modulating neuronal firing activities. In this paper, we found that the inhibitory autapse with delay can also induce MMOs and resting state to suppress repetitive firing. The results extend the formation condition of MMOs in biology and provide the potential functions of the inhibitory autapse in nervous systems. Similar to the study [10] in which excitatory autapse induced MMOs, the MMOs induced by inhibitory autapse depend on the dynamics of unstable behaviors near subcritical Hopf bifurcation, i.e., the slow repelling manifold of the unstable limit cycle or focus. Moreover, the generation of resting state depends on the bistable behaviors of the spiking and resting state. Although both the inhibitory and excitatory autapses can induce MMOs and resting state, there is a distinction. The inhibitory autaptic current plays negative effect on membrane potential, and the excitatory autaptic current provides positive effect. For the excitatory autapse, MMOs can be induced only when the excitatory autaptic current is applied at the after-hyperpolarization phase of a spike, and for the inhibitory autapse, only when the inhibitory autaptic current is applied at the depolarization phase of the next spike. The depolarization phase is behind the after-hyperpolarization phase. Thus, the time delay of the inhibitory autapse to induce MMOs or resting state is larger than that of the excitatory autapse.

The results of the present paper indicate that the inhibitory autapse can induce diverse dynamical behaviors to suppress firing activity, which depends on the negative effect of the inhibitory autaptic current and dynamical behaviors near the subcritical Hopf bifurcation. The subcritical Hopf bifurcation has been identified in several neuronal models, including the conductance-based Connor-Stevens, Morris-Lecar models, and dimensionless FitzHugh-Nagumo and Izhikevich models. The results of the present paper are applicable to these neuronal models. Electrophysiological experiments have shown that various neurons such as entorhinal cortex, neocortex and dopamine neurons exhibit class II excitability [30]. This paper shows the potential role of the inhibitory autapse whereby it can control neuronal firing patterns with the aid of the subcritical Hopf bifurcation. In the previous study [10] and this paper, the suppression effects of inhibitory and excitatory autapses are shown, and the dynamical mechanism of the suppression effects is identified through analyzing the changes of dynamical behav-

iors. These results present potential roles of inhibitory and excitatory autapses that can control firing patterns and firing rates related to neural code. For example, the firing rate of neurons with subcritical Hopf bifurcation is usually in a narrow high frequency band, however, the inhibitory and excitatory autapses can lower the firing rate of the neurons through the suppression effects, which may enhance the ability of the neurons to encode in a wider frequency band. Moreover, the different firing frequencies of neurons are implicated in different physiological processes. For instance, low-frequency firing activities and high-frequency firing activities of neurons in hippocampus appear in learning new information and consolidating memories, respectively [14, 30].

Acknowledgments

The authors are supported by the Science and Technology Project of Guangzhou (Grant No. 202102021167), the GDAS' Project of Science and Technology Development (Grant No. 2021GDASYL-20210103088),the National Natural Science Foundation of China (Grant No. 11802085), the Science and Technology Development Program of Henan Province (Grant No. 212102310827).

The authors would like to thank Prof. Gu Huaguang very much for his invaluable suggestions, and thank all the reviewers for their constructive comments.

Conflict of interest

The authors declare there is no conflicts of interest.

References

1. M. Desroches, J. Guckenheimer, B. Krauskopf, C. Kuehn, H. M. Osinga, M. Wechselberger, Mixed-mode oscillations with multiple time scales, *SIAM Rev.*, **54** (2012), 211–288. https://doi.org/10.1137/100791233
2. E. M. Izhikevich, Neural excitability, spiking and bursting, *Int. J. Bifurcat. Chaos*, **10** (2000), 1171–1266.
3. B. J. Bacak, T. Kim, J. C. Smith, J. E. Rubin, I. A. Rybak, Mixed-mode oscillations and population bursting in the pre-Bötzinger complex, *eLife*, **5** (2016), e13403. https://doi.org/10.7554/eLife.13403
4. C. Iglesias, C. Meunier, M. Manuel, Y. Timofeeva, N. Delestrée, D. Zytnicki, Mixed mode oscillations in mouse spinal motoneurons arise from a low excitability state, *J. Neurosci.*, **31** (2011), 5829–5840. https://doi.org/10.1523/JNEUROSCI.6363-10.2011
5. H. G. Rotstein, M. Wechselberger, N. Kopell, Canard induced mixed-mode oscillations in a medial entorhinal cortex layer II stellate cell model, *SIAM J. Appl. Dyn. Syst.*, **7** (2008), 1582–1611. https://doi.org/10.1137/070699093
6. M. Desroches, B. Krauskopf, H. M. Osinga, Numerical continuation of canard orbits in slow-fast dynamical systems, *Nonlinearity*, **23** (2010), 739–765. https://doi.org/10.1088/0951-7715/23/3/017

7. J. Y. Zhao, D. G. Fan, Q. S. Wang, Dynamical transitions of the coupled Class I (II) neurons regulated by an astrocyte, *Nonlinear Dynam.*, **103** (2021), 913–924. https://doi.org/10.1007/s11071-020-06122-3
8. Y. R. Liu, S. Q. Liu, Canard-induced mixed-mode oscillations and bifurcation analysis in a reduced 3D pyramidal cell model, *Nonlinear Dyn.*, **101** (2020), 531–567.
9. E. N. Davison, Z. Aminzare, B. Dey, N. E. Leonard, Mixed mode oscillations and phase locking in coupled FitzHugh-Nagumo model neurons, *Chaos*, **29** (2019), 033105. https://doi.org/10.1063/1.5050178
10. Z. G. Zhao, L. Li, H. G. Gu, Excitatory autapse induces different cases of reduced neuronal firing activities near Hopf bifurcation, *Commun. Nonlinear Sci. Numer. Simul.*, **85** (2020), 105250. https://doi.org/10.1016/j.cnsns.2020.105250
11. R. A. Silver, Neuronal arithmetic, *Nat. Rev. Neurosci.*, **11** (2010), 474–489. https://doi.org/10.1038/nrn2864
12. C. Van Vreeswijk, L. F. Abbott, G. B. Ermentrout, When inhibition not excitation synchronizes neural firing, *J. Comput. Neurosci.*, **1** (1994), 313–321. https://doi.org/10.1007/BF00961879
13. R. Dodla, G. Svirskis, J. Rinzel, Well-timed, brief inhibition can promote spiking: Postinhibitory facilitation, *J. Neurophysiol.*, **95** (2006), 2664–2677.
14. A. Bacci, J. R. Huguenard, D. A. Prince, Modulation of neocortical interneurons: extrinsic influences and exercises in self-control, *Trends Neurosci.*, **28** (2005), 602–610. https://doi.org/10.1016/j.tins.2005.08.007
15. L. P. Yin, R. Zheng, W. Ke, Q. S. He, Y. Zhang, J. L. Li, et al., Autapses enhance bursting and coincidence detection in neocortical pyramidal cells, *Nat. Commun.*, **9** (2018), 4890. https://doi.org/10.1038/s41467-018-07317-4
16. R. Saada, N. Miller, I. Hurwitz, A. J. Susswein, Autaptic excitation elicits persistent activity and a plateau potential in a neuron of known behavioral function, *Curr. Biol.*, **19** (2009), 479–484. https://doi.org/10.1016/j.cub.2009.01.060
17. L. L. Colgin, Rhythms of the hippocampal network, *Nat. Rev. Neurosci.*, **17** (2016), 239–249. https://doi.org/10.1038/nrn.2016.21
18. M. Y. Ge, Y. Xu, Z. K. Zhang, Y. X. Peng, W. J. Kang, L. J. Yang, et al., Autaptic modulation-induced neuronal electrical activities and wave propagation on network under electromagnetic induction, *Eur. Phys. J. Special Topics*, **227** (2018), 799–809. https://doi.org/10.1140/epjst/e2018-700141-7
19. H. X. Qin, J. Ma, W. Y. Jin, C. N. Wang, Dynamics of electric activities in neuron and neurons of network induced by autapses, *Sci. China Technol. Sci.*, **57** (2014), 936–946. https://doi.org/10.1007/s11431-014-5534-0
20. H. T. Wang, L. F. Wang, Y. L. Chen, Y. Chen, Effect of autaptic activity on the response of a Hodgkin-Huxley neuron, *Chaos*, **24** (2014), 033122. https://doi.org/10.1063/1.4892769
21. H. T. Wang, J. Ma, Y. L. Chen, Y. Chen, Effect of an autapse on the firing pattern transition in a bursting neuron, *Commun. Nonlinear Sci. Numer. Simul.*, **19** (2014), 3242–3254. https://doi.org/10.1016/j.cnsns.2014.02.018

22. D. Q. Guo, S. D. Wu, M. M. Chen, M. Perc, Y. S. Zhang, J. L. Ma, et al., Regulation of irregular neuronal firing by autaptic transmission, *Sci. Rep.*, **6** (2016), 26096. https://doi.org/10.1038/srep26096

23. V. Baysal, E. Erkan, E. Yilmaz, Impacts of autapse on chaotic resonance in single neurons and small-world neuronal networks, *Phil. Trans. R. Soc. A*, **379** (2021), 20200237. https://doi.org/10.1098/rsta.2020.0237

24. Z. G. Zhao, H. G. Gu, Transitions between classes of neuronal excitability and bifurcations induced by autapse, *Sci. Rep.*, **7** (2017), 6760. https://doi.org/10.1038/s41598-017-07051-9

25. X. L. Song, H. T. Wang, Y. Chen, Autapse-induced firing patterns transitions in the Morris-Lecar neuron model, *Nonlinear Dyn.*, **96** (2019), 2341–2350. https://doi.org/10.1007/s11071-019-04925-7

26. Z. G. Zhao, L. Li, H. G. Gu, Y. Gao, Different dynamics of repetitive neural spiking induced by inhibitory and excitatory autapses near subcritical Hopf bifurcation, *Nonlinear Dyn.*, **99** (2020), 1129–1154. https://doi.org/10.1007/s11071-019-05342-6

27. B. Cao, L. N. Guan, H. G. Gu, Bifurcation mechanism of not increase but decrease of spike number within a neural burst induced by excitatory effect, *Acta Phys. Sin.*, **67** (2018), 240502.

28. Y. Y. Li, H. G. Gu, X. L. Ding, Bifurcations of enhanced neuronal bursting activities induced by the negative current mediated by inhibitory autapse, *Nonlinear Dyn.*, **97** (2019), 2091–2105. https://doi.org/10.1007/s11071-019-05106-2

29. B. Ermentrout, *Simulating, analyzing, and animating dynamical systems: a guide to XPPAUT for researchers and students*, Society for Industrial and Applied Mathematics, PA, 2002.

30. R. A. Tikidji-Hamburyan, J. J. Martínez, J. A. White, C. C. Canavier, Resonant interneurons can increase robustness of gamma oscillations, *J. Neurosci.*, **35** (2015), 15682–15695. https://doi.org/10.1523/JNEUROSCI.2601-15.2015

AIMS Press